Myocardial energetics is not compromised during compensated hypertrophy in the Dahl salt-sensitive rat model of hypertension

K. Tran[1*], J-C. Han[1], A.J. Taberner[1,2], C.J. Barrett[2], E.J. Crampin[4,5,6], D.S. Loiselle[1,3]

[1]Auckland Bioengineering Institute, University of Auckland, Auckland, New Zealand

[2]Department of Engineering Science, University of Auckland, Auckland, New Zealand

[3]Department of Physiology, University of Auckland, Auckland, New Zealand

[4]Systems Biology Laboratory, Melbourne School of Engineering, University of Melbourne, Parkville, Victoria, Australia

[5]School of Mathematics and Statistics, University of Melbourne, Parkville, Victoria, Australia

[6]School of Medicine, University of Melbourne, Parkville, Victoria, Australia

* Corresponding author:

Email: k.tran@auckland.ac.nz (KT)

Abstract

Salt-induced hypertension leads to development of left-ventricular hypertrophy in the Dahl salt-sensitive (Dahl/SS) rat. Before progression to left-ventricular failure, the heart initially undergoes a compensated hypertrophic response. We hypothesized that changes in myocardial energetics may be an early indicator of transition to failure. Dahl/SS rats and their salt-resistant consomic controls (SS-13^{BN}) were placed on either a low- or high-salt diet to generate four cohorts: Dahl-SS rats on a low- (Dahl-LS) or high-salt diet (Dahl-HS) and SS-13^{BN} rats on a low- (SSBN-LS) or high-salt diet (SSBN-HS). We isolated left-ventricular trabeculae and characterized their mechano-energetic performance. Our results show, at most, modest effects of salt-induced compensated hypertrophy on myocardial energetics. We found that the Dahl-HS cohort had a higher work-loop heat of activation, (estimated from the intercept of the heat versus relative afterload relationship generated from work-loop contractions) relative to the SSBN-HS cohort and a higher economy of contraction (inverse of the slope of the heat versus active stress relation) relative to the Dahl-LS cohort. The maximum extent of shortening and maximum shortening velocity of the Dahl/SS groups were higher than those of the SS-13^{BN} groups. Despite these differences, no significant effect of salt-induced hypertension was observed for either peak work output or peak mechanical efficiency during compensated hypertrophy.

New and Noteworthy

A high salt diet promotes systemic hypertension, which leads the heart to undergo hypertrophy that may progress to failure. We have performed a systematic study on a salt-sensitive rat model of hypertension, which rules out mechano-energetic changes that were previously implicated in the progression to heart failure.

Introduction

In salt-sensitive individuals, a diet high in salt promotes systemic hypertension. The heart responds to the increased load by undergoing hypertrophy that is initially compensatory but eventually leads to dilated left-ventricular failure. Changes that occur in the compensated hypertrophic state thus provide early insights into the progression of pathological events that lead to heart failure.

In studies of hypertrophied myocytes from Dahl S rats fed a high-salt diet, negligible change is observed in excitation-contraction processes and contraction kinetics during compensated hypertrophy (13). Evidence from isolated papillary muscles further shows no change of magnitudes in either isometric stress production (7, 11, 15) or the Ca^{2+} transient (15). These data suggest that salt-induced compensated hypertrophy is not associated with dysfunction in either mechanics or Ca^{2+} dynamics.

What then might be the early change responsible for progression to LV failure? We hypothesize that compensated hypertrophy is characterized by disturbed myocardial energetics. Our hypothesis stems from a study by Morii et al. (12), who, in isolated whole-heart experiments, revealed an increase in the energetic cost of excitation-contraction coupling in compensated hypertrophy, as indicated by a higher VO_2-PVA intercept. Yet, in the same year, this change in energy utilization was not observed by Kameyama et al. (9). We suspect the apparent difference is because Morii et al. (12) controlled only for salt-resistance (comparing Dahl S rats with their salt-resistant controls, Dahl R, both of which were fed a high-salt diet) whereas Kameyama et al. (9) controlled only for dietary salt content (comparing low- and high-salt diets in Dahl S rats). Despite their conflicting results on the effect of high-salt diet on energetics, both studies reported no change in myocardial efficiency, quantified using the phenomenological 'pressure-volume area' concept. However, efficiency derived from the slope of the VO_2-PVA relationship includes a non-work term in the numerator (6) and is therefore not a thermodynamically consistent measure of mechanical efficiency (the ratio of mechanical work output to change of enthalpy).

In our study, we tested whether myocardial energetics, and in particular, mechanical efficiency is disturbed during compensated hypertrophy induced by a high-salt diet. As distinct from the Morii et al. (12) and Kameyama et al. (9) studies, we used four cohorts to control for both salt-resistance and salt intake. These were Dahl/SS rats exposed to a low- (Dahl-LS) or high-salt diet (Dahl-HS) and their respective salt-resistant consomic counterparts (SSBN-LS and SSBN-HS). We characterized the force development, shortening dynamics and heat production of isolated left-ventricular trabeculae from each of these cohorts to investigate the sources of impaired energetics during high-salt induced compensated hypertrophy.

Methods

Ethical approval

All experiments were conducted in accord with protocols approved by the University of Auckland Ethics committee (Approval R939).

Animals

Experiments were performed on an inbred line of Dahl salt-sensitive rats, Dahl/SS (SS/JrHsdMcwiCrl), and their salt-resistant consomic controls, SS-13^{BN} (SS-Chr 13^{BN}/McwiCrl). The animals were imported from Charles River (Massachusetts, USA) and housed in the Vernon Jansen Unit (animal facility) at the School of Medicine, University of Auckland. The consomic SS-13^{BN} rats are 98% identical to the Dahl/SS rats and differ only by introgression of chromosome 13 from the Brown Norway strain (2, 3). This chromosome contains a subset of genes that restore normal regulation to the renin-angiotensin system (RAS). Animals from both genetic lines were randomly assigned to either a low- or a high-salt diet. This generated four cohorts: Dahl-SS rats on a low- (Dahl-LS) or high-salt diet (Dahl-HS) and SS-13^{BN} rats on a low- (SSBN-LS) or high-salt diet (SSBN-HS).

Dietary regimes

The rats were maintained on either the high-salt AIN-76A diet (4% NaCl) imported from Dyets (Bethlehem, Philadelphia) or the low-salt 2018S diet (0.2% NaCl) imported from Harlan Teklad (Wisconsin, USA). The Teklad 2018S diet did not contain any food products of animal origin and was made from ground wheat and corn. Both diets consisted of approximately the same percentage of protein (18-20%) and fat (5-6%) although the AIN-76A diet had a higher percentage of carbohydrate (68% vs. 44%) and lower percentage of fiber (5% vs. 18%). The diets differed in their source of protein (casein in AIN-76A versus corn and wheat protein in 2018S), carbohydrate (sucrose and corn starch in AIN-76A versus. corn and wheat flour in 2018S) and fat (corn oil in AIN-76A versus soybean oil in 2018S). Following weaning, at 3 weeks of age, the animals were placed on either the high-salt

(AIN-76A) diet or the low-salt (Teklad 2018S) diet until sacrifice at 12-14 weeks of age. They had *ad lib* access to the food and water. The parental colony was maintained on the 2018S diet.

In vivo blood pressure measurement

For each cohort, 4 rats were randomly selected for *in vivo* telemetric measurement of blood pressure. Under sterile conditions, each rat was surgically implanted with a blood pressure telemeter (Model TRM53P, Millar, Auckland, NZ) with a solid- state pressure sensor at the tip of the catheter. The abdominal aorta was cannulated 1 cm-2 cm rostral to the iliac bifurcation and the sensor tip of the telemeter advanced proximally 1 cm-2 cm. Pain relief/analgesia (Temgesic, 20 mg/kg) and antibiotic (Baytril 2.5% solution, 0.8 mL/kg) were administered at the time of the surgery.

The arterial pressure signal was sampled at 500 Hz using an analogue-to-digital data acquisition card (PCI 6024E, National Instruments, TX, USA) and continuously displayed by a data acquisition program (Universal Acquisition 11, University of Auckland, Auckland, NZ). Heart rate and systolic and diastolic blood pressures were derived from the arterial pressure waveform. For calculation of the overall average level of mean arterial blood pressure, the sampled signals were averaged every 2 s. All subsequent data collection and analyses were performed using the same data analysis program. The telemeters were implanted at 12 weeks of age and blood pressure data were recorded for 2 weeks post-surgery; data from the second week are presented. One of the rats from the SSBN-LS cohort did not survive surgery.

Preparation of trabeculae

Each rat was deeply anesthetized with isofluorane (5% in O_2) and injected with heparin (1000 IU kg^{-1}). Following cervical dislocation, the heart and lungs were excised and quickly placed into chilled Tyrode solution. The aorta was immediately cannulated for Langendorff perfusion with, low-Ca^{2+} Tyrode solution (in mmol L^{-1}: 130 NaCl, 6 KCl, 1 $MgCl_2$, 0.5 NaH_2PO_4, 0.3 $CaCl_2$, 10 HEPES, 10

glucose; 20 BDM, pH adjusted to 7.4 by addition of Tris,) which was vigorously gassed with 100% O_2 at room temperature. Using a dissecting microscope, the left ventricle was cut open and trabeculae were isolated from the inner walls and individually mounted in a work-loop calorimeter (14). In the calorimeter, the trabecula was superfused (at a rate of 0.5 μL s^{-1}–0.7 μL s^{-1}) with normal Tyrode solution (composition as listed, above, except for a higher concentration of $CaCl_2$:1.5 mmol L^{-1} and without BDM) at 32 °C. It was then electrically stimulated to contract at 3 Hz (using 3 V, 3 ms pulses) for at least 30 min before it was gradually stretched to optimal length (L_o; the length that maximizes developed force). At L_o, the length and diameter of the trabecula were then measured using a microscope graticule. The cross-sectional area of each trabecula was calculated assuming a circular cross-section, and is used in the calculation of muscle stress (force per cross-sectional area, mimicking wall tension in the whole heart).

Experimental protocol

Each trabecula was first subjected to a series of seven after-loaded work-loop contractions (in order of decreasing afterload), starting from its preload at L_o. Force-length work-loops mimic pressure-volume loops of the heart (14). For each afterloaded work-loop, steady-state was reached after approximately 2-3 min. Between each of the seven work-loops, the muscle was returned to L_o where it contracted isometrically for 2-3 min (a typical record is shown in Figure 4). This was necessary to ensure that muscle performance was not compromised upon changing muscle length during work-loop contractions, and to allow comparison of the base-line value for the rate of heat production between work-loop contractions. Upon completion of the work-loop protocol, each trabecula was subjected to a series of isometric contractions at seven different preloads, commencing at L_o and proceeding to a slack length where almost no active force was produced. Steady-state force and rate of heat production were reached for each of the pre-loaded isometric contractions (a typical record is shown in Figure 1). We estimate Activation Enthalpy (energy associated with the triggering of contraction) in two distinct ways: (i) by extrapolation of the

isometric heat-stress relation to the zero stress (isometric heat of activation) and (ii) by extrapolation of the work-loop heat-afterload relation to zero afterload (work-loop heat of activation). Note that both of these estimates avoid contamination with Basal Enthalpy.

Data recording and analysis

Measurements of force, length and rate of heat production were recorded throughout an experiment using LabView (National Instruments). Data from the work-loop protocol were analyzed (using MatLab) to derive the steady-state force-length work output (calculated as the area within a work-loop), work-loop heat output, extent of shortening (width of work-loop), maximal velocity of shortening (the maximal slope of the length-time trajectory during shortening), and mechanical efficiency (the ratio of work to the sum of work and heat). Similarly, data from the isometric protocol were analyzed to derive the steady-state isometric force production, twitch duration, maximal rates of rise and fall of the twitch, force-time integral and isometric heat production.

Corrections for thermal artefacts

The cyclic movement of the upstream hook (required to change the length of the trabecula to perform work-loop contractions) introduced a heat artefact. Upon completion of the work-loop and isometric protocols, stimulation was turned off and the trabecula was quiescent. The heat artefact induced by the movement of the upstream hook was determined by oscillating the hook at a frequency of 3 Hz and a magnitude equal to the maximal extent of shortening of the trabecula. A second source of heat artefact, arising from electrical stimulation, was determined by applying the stimulus in the absence of the trabecula. Net muscle heat output was corrected for both heat artefacts.

Statistical analyses

The functions used to fit the data are detailed in the figure captions. In general, data were fitted using polynomial regressions (up to third-order). A lower order polynomial was favored if an F-test detected no statistical improvement compared to a higher-order polynomial. Regression lines (fitted to data from individual trabecula) were averaged within groups using the "random coefficient" model within the *Proc Mixed* procedure of SAS. The significance of differences among regression lines of the 4 rat groups was tested using a set of orthogonal contrast vectors: [1 -1 0 0], [0 0 1 -1] and [1 1 -1 -1]. Parameters of interest arising from the work-loop protocols (peak values of shortening, shortening velocity, shortening power, work, mechanical efficiency and heat at peak mechanical efficiency) were extracted from the appropriate regression line. They were then averaged and compared among the 4 groups using analysis of variance within the 'Generalized Linear Model' of SAS. The same set of orthogonal contrast vectors as above was used in post-hoc tests. In all cases, statistical significance was declared when $p < 0.05$.

Results

In vivo blood pressure

Dahl/SS rats on the high-salt diet (Dahl-HS) had greater average values of systolic and diastolic and mean blood pressures compared with their low-salt controls (Table 1). The hypertensive effect of the high-salt diet was observed only in the Dahl/SS strain and not the salt-resistant SS-13^{BN} strain, suggesting the effectiveness of chromosome 13 in protecting these hearts from developing hypertension. The average heart rates did not differ among the 4 groups.

Morphometric characteristics of the rats

All 4 groups of animals reached a similar size upon sacrifice at 12-14 weeks of age (Table 1). The Dahl-LS group attained a higher body weight than the Dahl-LS group despite having marginally lower tibial length. Compared with their respective controls, the two high-salt diet groups had larger average heart masses and larger average ventricular masses. The ventricular mass was approximately 30% greater in the Dahl-HS group compared to its low-salt control, while the increase between the two SS-13^{BN} groups was only 17%. The Dahl-HS group also had 20% thicker left ventricular walls relative to Dahl-LS but a comparable difference was not seen between the two SS-13^{BN} groups. Overall, these results clearly show that the high-salt diet caused significant left ventricular hypertrophy in the Dahl/SS strain but not in the salt-resistant SS-13^{BN} strain.

Trabecula dimensions

There were no differences in the mean diameters or lengths of trabeculae between the high-salt groups and their low-salt controls (Table 1). However, on average, trabeculae dissected from the SS-13^{BN} salt-resistant strain were longer than those from the Dahl/SS strain.

Isometric contractions

Twitch profiles of a trabecula contracting isometrically at decreasing muscle lengths are shown in Figure 1A. Total stress and passive stress as functions of relative muscle length are plotted, along with their averaged regression lines (Figure 1B). Although the stress-length relationship of the Dahl-HS group appears to be higher than those of the other three groups, no statistically significant effect of a high-salt diet or salt-resistance was detected. The average peak values of total stresses at optimal length ($L/L_o = 1$) also did not differ among groups (Dahl-LS: 63.5 kPa ± 6.5 kPa; Dahl-HS: 73.8 kPa ± 6.6 kPa; SSBN-LS: 72.4 kPa ± 8.1 kPa; SSBN-HS: 68.0 kPa ± 10.2 kPa). Figure 1C shows the heat generated from isometric contractions by a representative trabecula.

Characteristics of the twitch profile were examined to ascertain any effect of a high-salt diet or salt resistance (Figure 2). The twitch duration at 5% and 50% of peak stress as a function of active stress (Figure 2A), the maximal rate of force development and relaxation as a function of active stress (Figure 2B) and the stress-time integral (STI) as a function of active stress did not differ among the four groups.

The rate of heat production (Figure 1C) was converted to heat per twitch by dividing by the stimulus frequency (3 Hz). Steady-state twitch heat as a function of active stress is shown in Figure 3A. The intercept of the heat-stress is an index of the isometric activation heat (attributed predominantly to SERCA activity). The inverse of the slope is an index of cross-bridge economy (force development per unit heat output) and is higher in the Dahl-HS than in the Dahl-LS groups (Figure 3B). No effects are observed on the isometric heat of activation among the 4 groups (Figure 3C).

Work-loop contractions

Figure 4A shows the work-loop twitch profiles where “A” indicates the isometric twitch (where the muscle was effectively contracting against an infinite afterload) and “I” labels the lowest afterload. The corresponding change in muscle length is plotted in Figure 4B. As afterload decreases, the extent of shortening increases. Parametric plots of the stress versus length profiles (Figure 4C) allow

258 quantification of external work output, given by the area within the stress-length loop. The rate of
259 heat production generated by each work-loop is shown in Figure 4D. Each work-loop contraction
260 was bracketed by an isometric contraction at L_o.
261 Muscle shortening characteristics during a work-loop protocol are shown in Figure 5. The relation
262 between the extent of shortening and relative afterload did not differ among the four groups (Figure
263 5A). However, there was an effect of salt resistance on the maximal extent of shortening; that is,
264 shortening at zero relative afterload (Figure 5D). Trabeculae from the Dahl/SS strain shortened to a
265 greater extent than those of the SS-13^{BN} strain. Similarly, no difference was detected in the relation
266 between velocity of shortening and relative active afterload (Figure 5B) but an effect of salt
267 resistance was found on the maximal velocity of shortening (which occurs at zero afterload: Figure
268 5E). The higher maximum velocity of shortening in the Dahl/SS strain is likely a corollary of their
269 greater extent of maximal shortening. The product of velocity of shortening and relative afterload
270 produces the power of shortening (Figure 5C). No differences were detected in the relation
271 between power of shortening and relative afterload or in the peak maximum power output (Figure
272 5F) among the 4 groups.
273 Simultaneous measurement of trabecula mechanics and heat output during a work-loop protocol
274 allows quantification of muscle work and mechanical efficiency (ratio of work to the sum of work
275 and heat). There were no differences in the relations between either work output (Figure 6A) or
276 mechanical efficiency (Figure 6C) and relative afterload among the four cohorts. Peak work output
277 (Figure 6D) and peak mechanical efficiency did not differ either (Figure 6F). There was, however, a
278 difference in the relations between heat and relative afterload between the two rat strains (Figure
279 6B). The difference was found to be attributed to the extrapolated intercept of the linear regression
280 curves (work-loop heat of activation) and not the slope. The work-loop heats of activation
281 (determined from the extrapolated intercepts of the heat versus relative afterload relations; Figure
282 6B) were higher in the Dahl-HS groups than in their consomic controls (Figure 6E).

It is of note that the work-loop heats of activation (Figure 6E) were, on average, twice as large as those measured from the isometric protocol (Figure 3C). This is consistent with an earlier study by Gibbs et al. (5), in which the estimated heat from a quick-release technique was also two-fold higher than that obtained from the gradual shortening protocol. We attribute the protocol-dependent differences in estimate of activation heat to the fact that, under both the quick-release and work-loop protocols, there is only a single preload and, hence, no opportunity for length-dependent Ca^{2+} effects to occur. By contrast, the gradual shortening of the isometric protocol requires the muscle to be equilibrated at a series of different preloads, allowing length-dependent activation to instantiate.

Discussion

This is the first study of the effect of high-salt induced compensated hypertrophy on myocardial energetics using ventricular trabeculae. The use of isolated trabeculae allows investigations to be performed over a complete range of muscle lengths (Figures 1-3) and afterloads (Figures 4-6), from which mechano-energetic performance can be characterized. A novelty of the present study resides in the comparison between Dahl/SS and their salt-resistant consomic controls (SS-13^{BN}), both groups being fed with both low- and a high-salt diets. This experimental design was chosen to resolve the apparently conflicting results between Morii et al. (12) and Kameyama et al. (9), the only two studies that have investigated the effects of high-salt diets on myocardial energetics.

Our results generally show at most modest effects of salt-induced compensated hypertrophy on myocardial energetics. This is clearly not a consequence of too brief a period of high salt intake since our Dahl/SS rats demonstrated undeniable systemic hypertension and compensated hypertrophy with no signs of heart failure (Table 1).

Other studies on the Dahl/SS rats have found that an exposure of three weeks (4, 10) is sufficient to elicit a hypertensive response (MAP>150 mmHg). In preliminary investigations (data not shown) we adopted the 3- week protocol, which resulted in an inadequate hypertensive response. Rather,

we found that 9 weeks of exposure was necessary to induce hypertension. The reason for this discrepancy we attribute to a difference of dietary exposure of the rats during their embryonic development. Thus, Geurts et al. (4) recently reported that Dahl/SS offspring, which had been exposed to a maternal diet of casein-based AIN-76A chow (low salt, 0.4% NaCl) during the periods of gestation and lactation, were more sensitive to high-salt than those that had been exposed to a grain-based maternal diet. These authors speculated that the maternal dietary exposures may have altered gene expression of the embryos. Our Dahl/SS colony was maintained on the Teklad 2018 grain-based diet. This is likely to account for the attenuated hypertensive response we saw when the Dahl/SS rats were exposed to only 3 weeks of high-salt. We were able to overcome this reduced salt-sensitivity by increasing the exposure to 9 weeks, which elicited a reasonable compensated hypertrophic response. Continued exposure of the Dahl/SS rat to a high-salt diet would progress the heart from compensated hypertrophy into dilated left ventricular hypertrophy (8). It is interesting to note that the MAP of the Dahl low-salt control group (Dahl-LS) was higher than that of the salt-resistant high-salt SSBN-HS group (Table 1), indicating that these rats were predisposed to hypertension and that high salt intake accelerated this development. This is unsurprising considering that the Dahl/SS rats have a disrupted RAS pathway due to the missing renin gene on chromosome 13, which is present in the salt-resistant SS-13^{BN} animals (1, 2).

Given the compensated hypertrophic response of our Dahl-HS animals, we sought to investigate mechano-energetic consequences on their trabecula tissue. Using our work-loop calorimeter, we characterized the mechanical performance and heat production from trabeculae undergoing both isometric and work-loop contractions. We found that there were no significant effects of a high-salt diet or salt-resistance on the steady-state isometric twitch profile (Figure 1B and Figure 2). The hypertensive response of the Dahl-HS hearts does not appear to instantiate in its trabecula tissue. This finding is consistent with reports on papillary muscles isolated from Dahl S animals on a high-salt diet, which showed (relative to their salt-resistant counterpart) no difference in peak isometric force production (7, 11, 15). In our case, not only was peak stress unchanged, but developed stress

as a function of the working range of muscle length was insensitive to salt-induced hypertension (Figure 1B). Our finding that there were no effects of a high-salt diet on the maximum rate of stress development and relaxation over the course of a twitch (Figure 2B) is also consistent with the absence of change in cross-bridge kinetics during compensated hypertrophy reported by McCurdy et al. (11). When the muscles were subjected to a work-loop protocol where they shortened against a series of afterloads, we found that the Dahl/SS strain (Dahl-LS & Dahl-HS) had a greater maximal extent of shortening (Figure 5D) and a higher maximal velocity of shortening (Figure 5E) than the salt-resistant strain (SSBN-LS + SSBN-HS). This suggests that the Dahl/SS strain had a higher *maximum* cross-bridge cycling rate which is independent of high-salt intake.

We found that the economy of contraction was higher for the Dahl-HS cohort when compared to its low-salt counterpart, Dahl-LS (Figure 3B). This is consistent with whole-heart data from Kameyama et al. (9) who also reported a higher economy (inverse of the slope of the VO_2-FTI integral relationship) for the high-salt Dahl S group. Increased economy indicates that less energy is consumed in order to generate a unit of active stress. The economy of contraction is modified by factors that alter either the energy requirements of cross-bridge cycling or its mechanical output. Our results on the rate of force development and relaxation indicate that the cross-bridge cycling kinetics are unchanged among the four cohorts (Figure 2B), although the Dahl/SS strain can achieve a higher maximal shortening velocity under zero load conditions (Figure 5B). We can therefore only speculate that there appears to be a favorable shift in the ratio of ATP consumed per unit of force produced in the compensated hypertrophied Dahl-HS rats.

In terms of mechano-energetic performance, we found that there were no significant differences in peak external work, heat output and peak mechanical efficiency among the four cohorts (Figure 6). However, we did find that the work-loop heat of activation was higher for the Dahl-HS group compared to its salt-resistant control (SSBN-HS), yet there was no difference between the Dahl-HS group and its salt diet control (Dahl-LS). This result resolves the apparent conflict between the reports of Morii et al. (12) and Kameyama et al. (9) in which the former showed a salt-induced

increase in work-independent energy while the latter did not. Both studies used isolated whole-hearts performing pressure-volume loops but Morii et al. (12) made a comparison between Dahl S rats and their salt-resistant control, Dahl R (both on high-salt diets) whereas Kameyama et al. (9) made a comparison between Dahl S rats on either a low- or high-salt diet. A difference to note in the comparison of our measured work-loop heat of activation to the reported work-independent energy utilization is that the latter includes the basal metabolism component in addition to the energetic cost of excitation-contraction. Our results provide direct estimates of the heat associated with the energetic cost of excitation-contraction coupling (attributed primarily to the SERCA pump). Thus, the activation heat is a reflection of the number of the calcium ions sequestered. Yoneda et al. (15) reported no change in the profile of Ca^{2+} transient as well as no differences in the rate of Ca^{2+} uptake by isolated papillary muscles between Dahl S and Dahl R rats on high-salt diets during compensated hypertrophy. This appears to contradict the results of Morii et al. (12) but the key difference is that the Yoneda et al. (15) study imposed an isometric protocol on isolated papillary muscles whereas the former used whole-heart contractions. Our estimate of isometric activation heat, estimated from the intercept of the heat versus active isometric stress relationship (Figure 3C), is consistent with the results of Yoneda et al. (15). Taken together, our results suggest that, under a work-loop protocol, a combination of salt-resistance and a high-salt diet may truncate the Ca^{2+} transient of the SSBN-HS, relative to that of the Dahl-HS cohort.

In conclusion, our extensive set of experimental measurements provides little evidence to support our initial hypothesis that compensated hypertrophy is characterized by disturbed myocardial energetics. In conjunction with the results of others who have shown comparably minor influence on the Ca^{2+}-transient, we conclude that the word ‘compensated’ in the phrase ‘compensated hypertrophy’ has been well chosen and that mechano-energetic status during this period gives us only the weakest hints of either the time-course or severity of subsequent developments in the pending phase of ‘cardiac failure’. Our study has highlighted the importance of controlling for both

genetically-conferred salt-resistance and environmentally driven salt intake thereby resolving an apparent conflict in the literature.

Grants

This work was supported by the Virtual Physiological Rat Centre funded through NIH grant P50-GM094503 (KT); Marsden Fund, from Government funding, administered by the Royal Society of New Zealand (AT); National Heart Foundation Fellowship grant and Royal Society of New Zealand Marsden Fast-start (JCH); and National Heart Foundation (DL).

References

1. **Amaral SL, Roman RJ, and Greene AS.** Renin gene transfer restores angiogenesis and vascular endothelial growth factor expression in Dahl S rats. *Hypertension* 37: 386-390, 2001.
2. **Cowley AW, Roman RJ, Kaldunski ML, Dumas P, Dickhout JG, Greene AS, and Jacob HJ.** Brown Norway chromosome 13 confers protection from high salt to consomic Dahl S rat. *Hypertension* 37: 456-461, 2001.
3. **Drenjancevic-Peric I and Lombard JH.** Introgression of chromosome 13 in Dahl salt-sensitive genetic background restores cerebral vascular relaxation. *American Journal of Physiology-Heart and Circulatory Physiology* 287: H957-H962, 2004.
4. **Geurts AM, Mattson DL, Liu P, Cabacungan E, Skelton MM, Kurth TM, Yang C, Endres BT, Klotz J, Liang M, and Cowley AW.** Maternal Diet During Gestation and Lactation Modifies the Severity of Salt-Induced Hypertension and Renal Injury in Dahl Salt-Sensitive Rats. *Hypertension* 65: 447-U451, 2015.
5. **Gibbs CL, Loiselle DS, and Wendt IR.** Activation heat in rabbit cardiac muscle. *Journal of Physiology-London* 395: 115-130, 1988.
6. **Han JC, Taberner AJ, Tran K, Goo S, Nickerson DP, Nash MP, Nielsen PMF, Crampin EJ, and Loiselle DS.** Comparison of the Gibbs and Suga formulations of cardiac energetics: the demise of "isoefficiency". *Journal of Applied Physiology* 113: 996-1003, 2012.
7. **Inoko M, Kihara Y, Morii I, Fujiwara H, and Sasayama S.** Transition from compensatory hypertrophy to dilated, failing left-ventricles in Dahl salt-sensitive rats. *American Journal of Physiology-Heart and Circulatory Physiology* 267: H2471-H2482, 1994.
8. **Iwanaga Y, Kihara Y, Hasegawa K, Inagaki K, Yoneda T, Kaburagi S, Araki M, and Sasayama S.** Cardiac endothelin-1 plays a critical role in the functional deterioration of left ventricles during the transition from compensatory hypertrophy to congestive heart failure in salt-sensitive hypertensive rats. *Circulation* 98: 2065-2073, 1998.
9. **Kameyama T, Chen ZY, Bell SP, VanBuren P, Maughan D, and LeWinter MM.** Mechanoenergetic alterations during the transition from cardiac hypertrophy to failure in Dahl salt-sensitive rats. *Circulation* 98: 2919-2929, 1998.
10. **Mattson DL, Kunert MP, Kaldunski ML, Greene AS, Roman RJ, Jacob HJ, and Cowley AW.** Influence of diet and genetics on hypertension and renal disease in Dahl salt-sensitive rats. *Physiological Genomics* 16: 194-203, 2004.
11. **McCurdy DT, Palmer BM, Maughan DW, and Lewinter MM.** Myocardial cross-bridge kinetics in transition to failure in Dahl salt-sensitive rats. *American Journal of Physiology-Heart and Circulatory Physiology* 281: H1390-H1396, 2001.
12. **Morii I, Kihara Y, Inoko M, and Sasayama S.** Myocardial contractile efficiency and oxygen cost of contractility are preserved during transition from compensated hypertrophy to failure in rats with salt-sensitive hypertension. *Hypertension* 31: 949-960, 1998.
13. **Nagata K, Liao RL, Eberli FR, Satoh N, Chevalier B, Apstein CS, and Suter TM.** Early changes in excitation-contraction coupling: transition from compensated hypertrophy to failure in Dahl salt-sensitive rat myocytes. *Cardiovascular Research* 37: 467-477, 1998.
14. **Taberner AJ, Han JC, Loiselle DS, and Nielsen PMF.** An innovative work-loop calorimeter for in vitro measurement of the mechanics and energetics of working cardiac trabeculae. *Journal of Applied Physiology* 111: 1798-1803, 2011.
15. **Yoneda T, Kihara Y, Ohkusa T, Iwanaga Y, Inagaki K, Takeuchi Y, Hayashida W, Ueyama T, Hisamatsu Y, Fujita M, Hatac S, Matsuzaki M, and Sasayama S.** Calcium handling and sarcoplasmic-reticular protein functions during heart-failure transition in ventricular myocardium from rats with hypertension. *Life Sciences* 70: 143-157, 2001.

Parameter	Dahl-LS	Dahl-HS	SSBN-LS	SSBN-HS
Age (weeks)	12.9 ± 0.2 (16)	13.7 ± 0.2 (12)*	13.6 ± 0.2 (11)	13.1 ± 0.1 (14)*
Body mass (g) #	410 ± 6 (16)	393 ± 9 (12)*	385 ± 5 (11)	382 ± 4 (14)
Tibial length (mm)	39.1 ± 0.2 (8)	39.8 ± 0.1 (10)*	39.5 ± 0.2 (11)	39.8 ± 0.2 (14)
Heart mass (g) #	1.50 ± 0.03 (12)	1.88 ± 0.05 (12)*	1.31 ± 0.01 (11)	1.46 ± 0.02 (14)*
Heart mass/body mass (%) #	0.37 ± 0.01 (12)	0.48 ± 0.02 (12)*	0.34 ± 0.01 (11)	0.38 ± 0.01 (14)*
Heart mass/tibial length (g/m) #	39.3 ± 0.8 (8)	47.6 ± 1.4 (10)*	33.2 ± 0.4 (11)	36.6 ± 0.5 (14)*
Ventricular mass (g) #	1.35 ± 0.03 (12)	1.74 ± 0.04 (12)*	1.19 ± 0.02 (11)	1.34 ± 0.02 (14)*
Ventricular mass/tibial length (g/m) #	35.3 ± 0.8 (8)	43.9 ± 1.3 (10)*	30.3 ± 0.4 (11)	33.6 ± 0.5 (14)*
LV thickness (mm) #	4.6 ± 0.1 (8)	5.5 ± 0.2 (12)*	4.5 ± 0.1 (11)	4.5 ± 0.1 (14)
LV thickness/tibial length (%) #	11.7 ± 0.3 (8)	14.1 ± 0.4 (10)*	11.3 ± 0.3 (11)	11.2 ± 0.2 (14)
Trabeculae dimensions				
Length (mm) #	2.72 ± 0.19 (19)	3.07 ± 0.19 (18)	3.30 ± 0.22 (14)	3.43 ± 0.19 (14)
Diameter (µm)	257 ± 16 (19)	242 ± 15 (18)	246 ± 30 (14)	259 ± 23 (14)
In vivo measurements				
Heart rate (beats/min)	339 ± 4 (4)	330 ± 6 (4)	343 ± 3 (3)	342 ± 4 (4)
Mean arterial pressure (mmHg) #	117 ± 3 (4)	137 ± 6 (4)*	103 ± 2 (3)	108 ± 1 (4)
Systolic arterial pressure (mmHg) #	144 ± 3 (4)	171 ± 6 (4)*	128 ± 2 (3)	138 ± 2 (4)
Diastolic arterial pressure (mmHg) #	97 ± 3 (4)	111 ± 5 (4)*	84 ± 1 (3)	84 ± 3 (4)

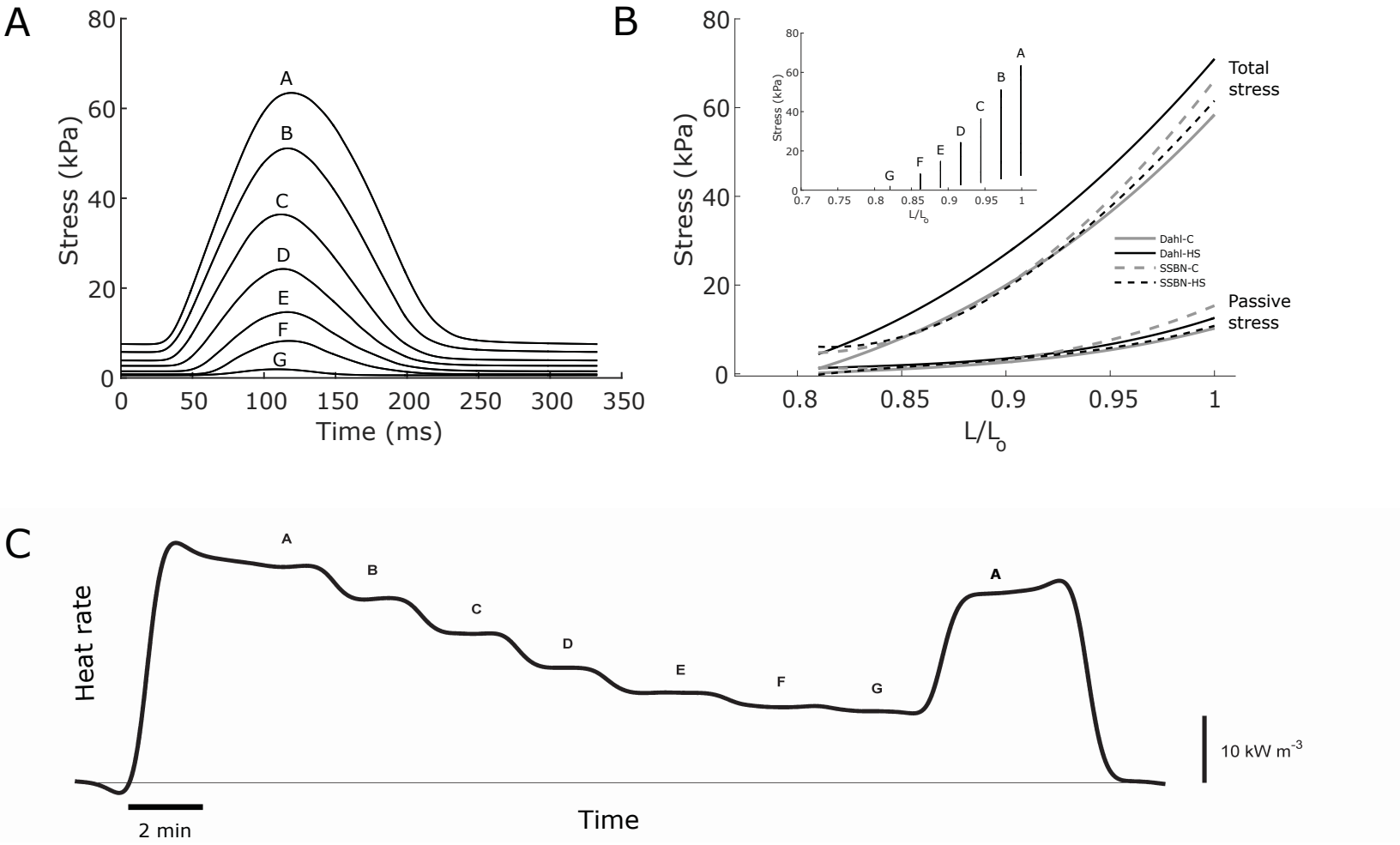
A
Stress (kPa)
Time (ms)
A
B
C
D
E
F
G
B
Stress (kPa)
L/L0
Total stress
Passive stress
Dahl-C
Dahl-HS
SSBN-C
SSBN-HS
C
Heat rate
Time
2 min
10 kW m-3

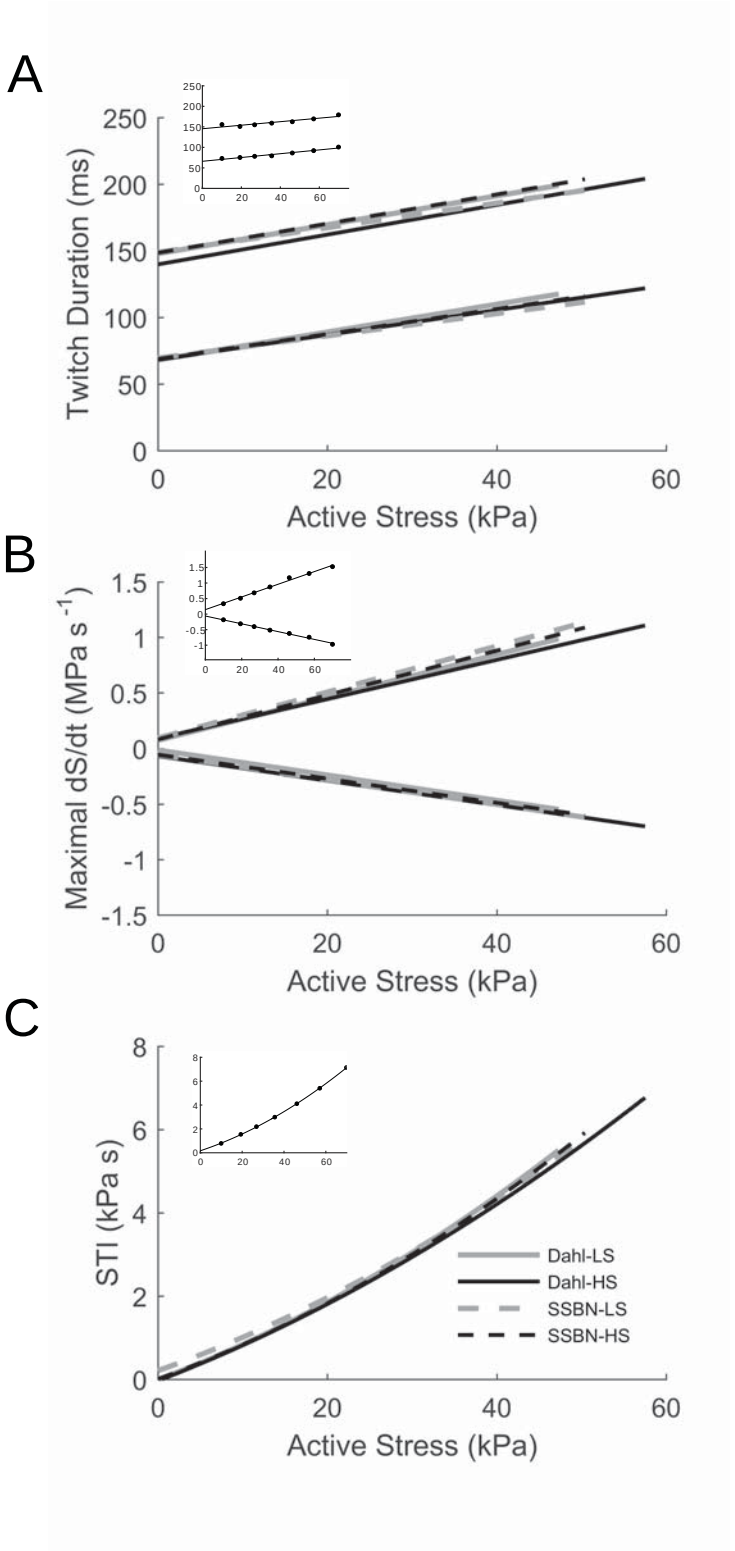
A
Twitch Duration (ms)
Active Stress (kPa)
B
Maximal dS/dt (MPa s-1)
Active Stress (kPa)
C
STI (kPa s)
Active Stress (kPa)
Dahl-LS
Dahl-HS
SSBN-LS
SSBN-HS

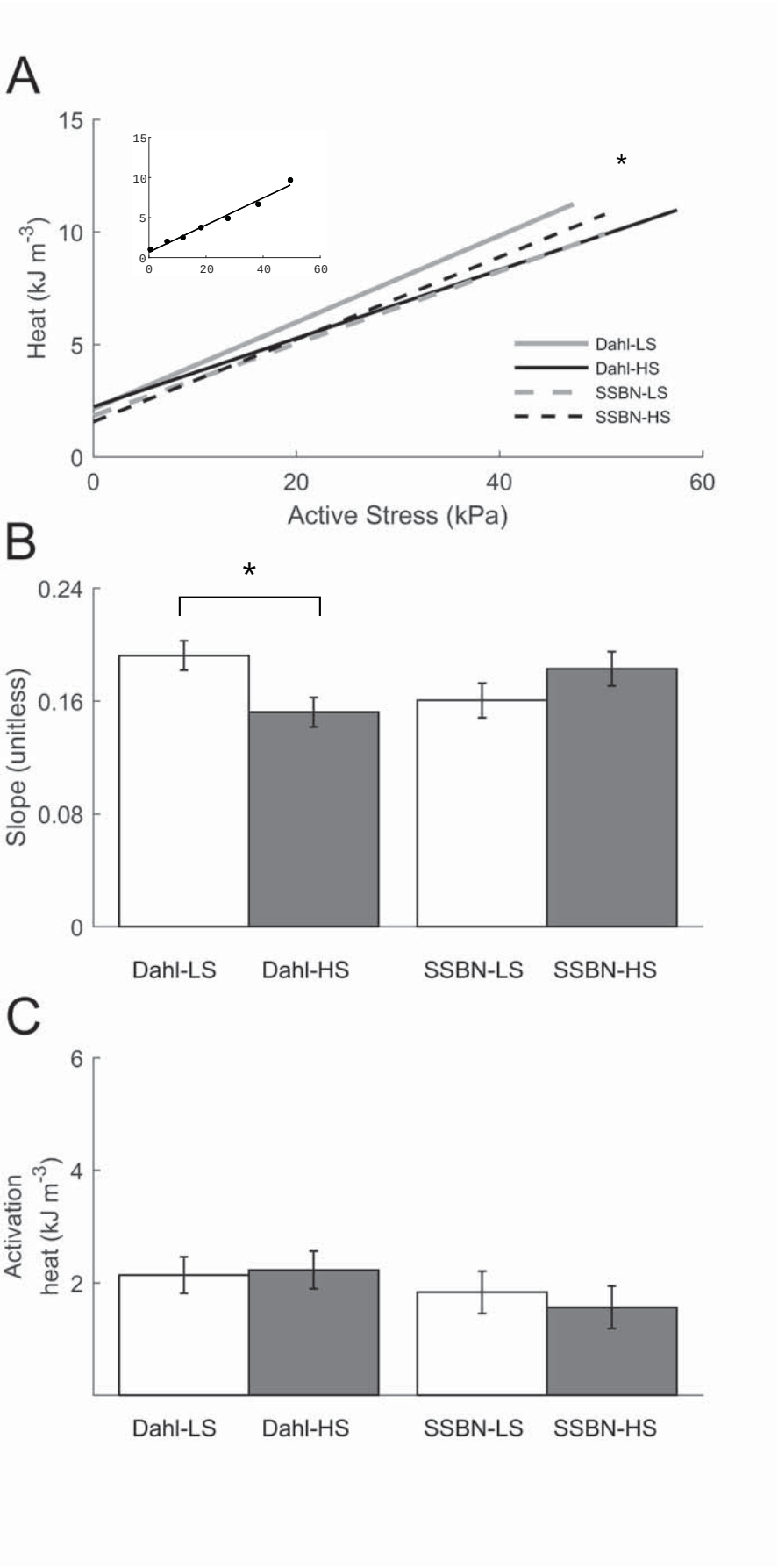
A
Heat (kJ m-3)
Active Stress (kPa)
Dahl-LS
Dahl-HS
SSBN-LS
SSBN-HS
*
B
Slope (unitless)
*
Dahl-LS
Dahl-HS
SSBN-LS
SSBN-HS
C
Activation heat (kJ m-3)
Dahl-LS
Dahl-HS
SSBN-LS
SSBN-HS

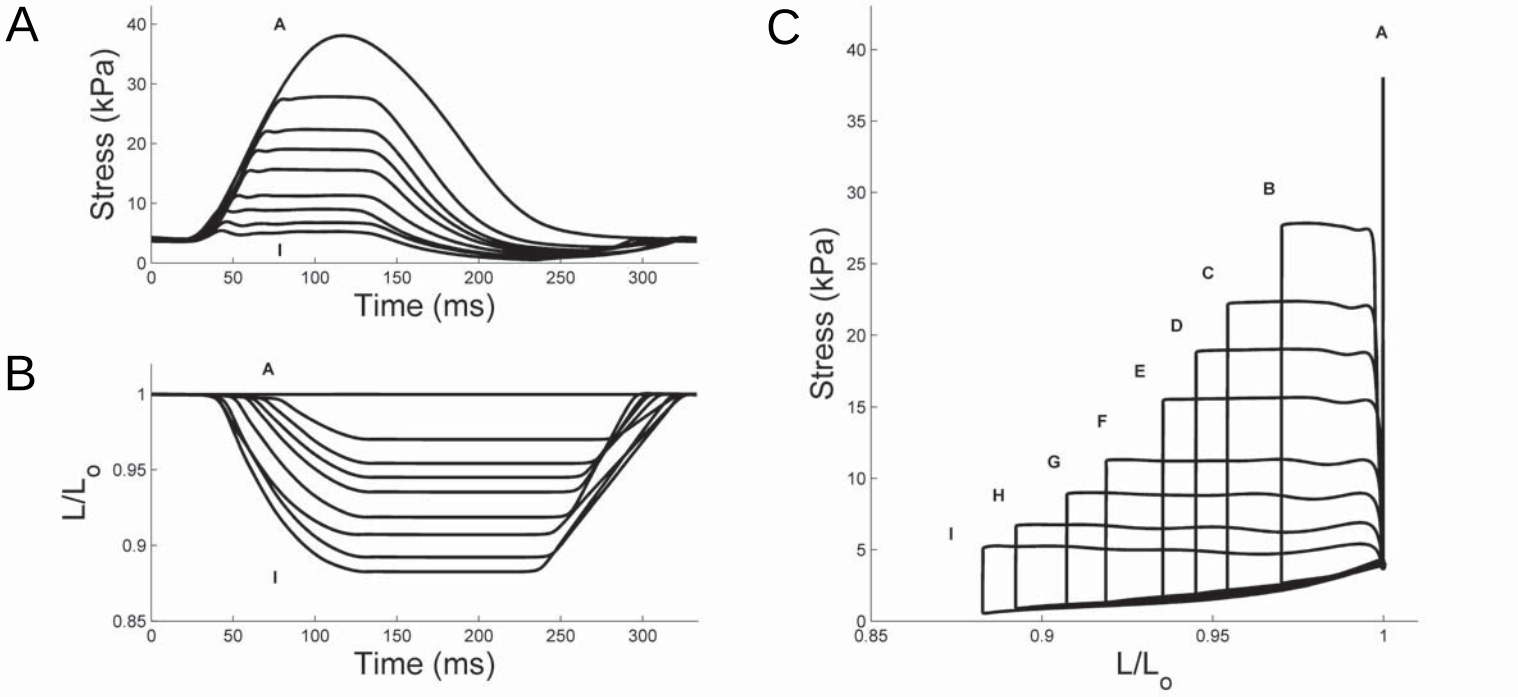
A
Stress (kPa)
Time (ms)
A
I
B
L/L$_o$
Time (ms)
A
I
C
Stress (kPa)
L/L$_o$
A
B
C
D
E
F
G
H
I

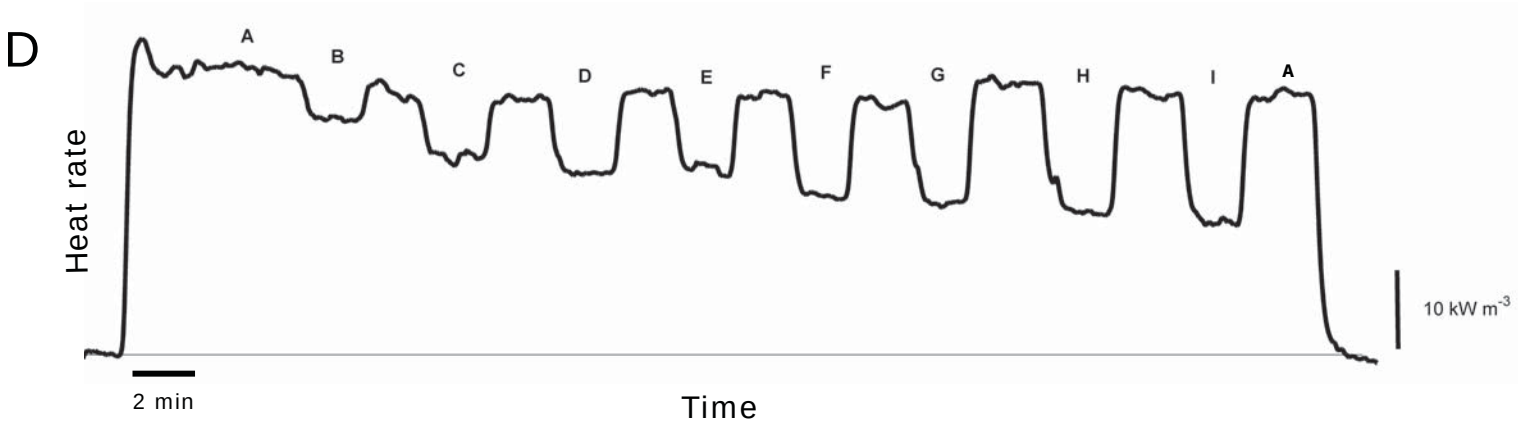
D
Heat rate
A
B
C
D
E
F
G
H
I
A
10 kW m^{-3}
2 min
Time

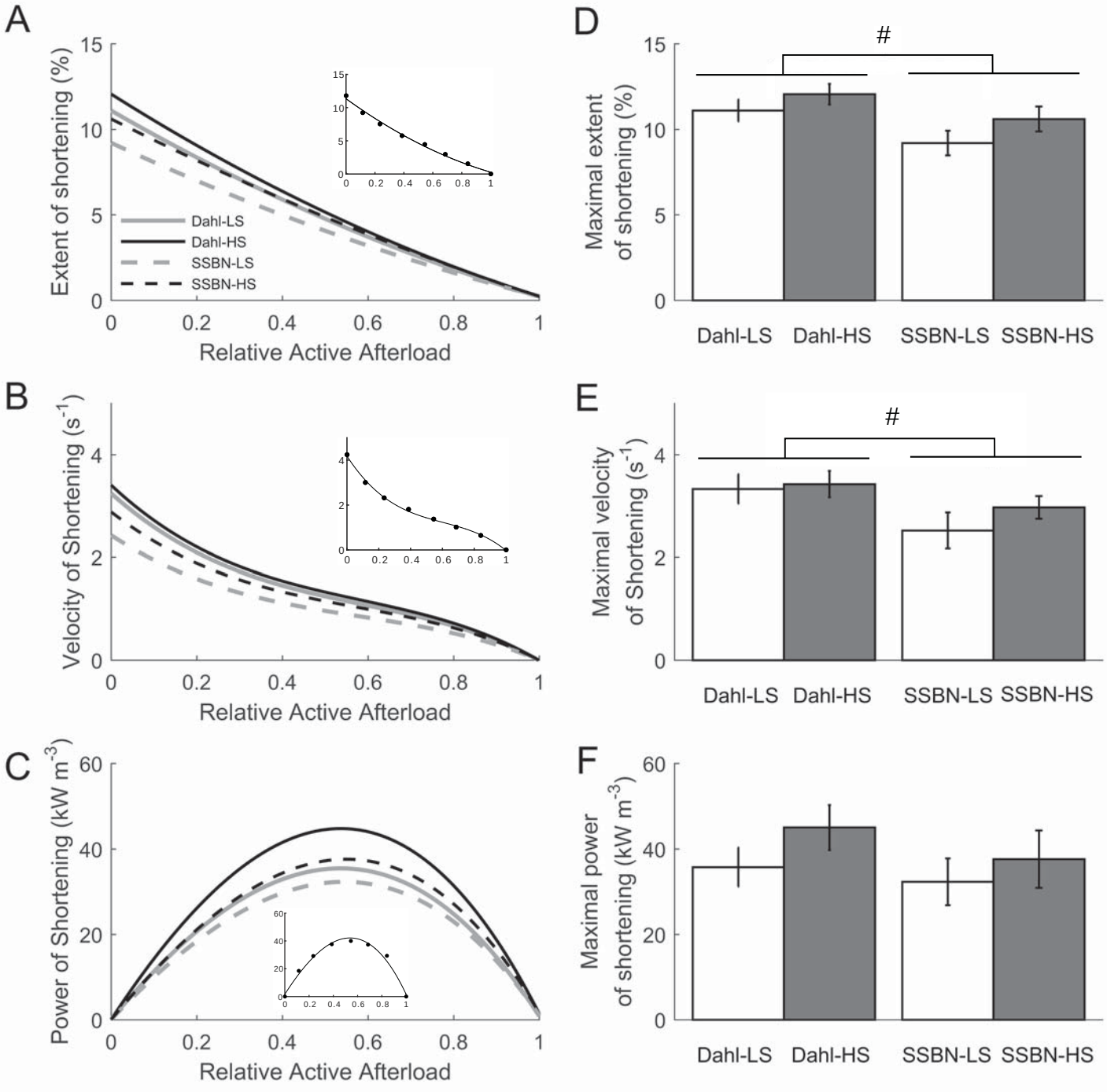
A
Extent of shortening (%)
Relative Active Afterload
Dahl-LS
Dahl-HS
SSBN-LS
SSBN-HS
B
Velocity of Shortening (s-1)
Relative Active Afterload
C
Power of Shortening (kW m-3)
Relative Active Afterload
D
Maximal extent of shortening (%)
#
Dahl-LS
Dahl-HS
SSBN-LS
SSBN-HS
E
Maximal velocity of Shortening (s-1)
#
Dahl-LS
Dahl-HS
SSBN-LS
SSBN-HS
F
Maximal power of shortening (kW m-3)
Dahl-LS
Dahl-HS
SSBN-LS
SSBN-HS

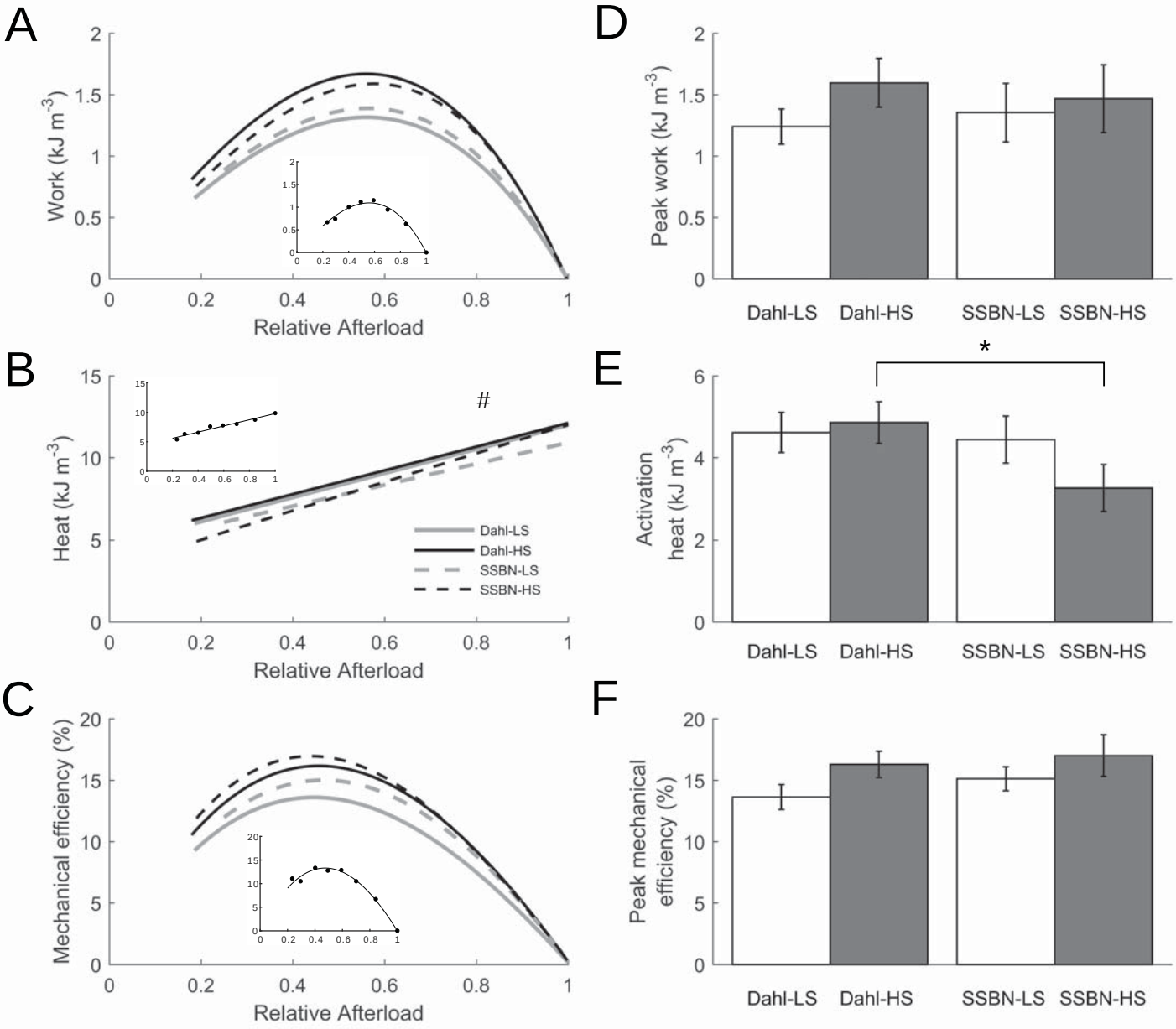
A
Work (kJ m-3)
Relative Afterload
B
Heat (kJ m-3)
#
Dahl-LS
Dahl-HS
SSBN-LS
SSBN-HS
Relative Afterload
C
Mechanical efficiency (%)
Relative Afterload
D
Peak work (kJ m-3)
Dahl-LS
Dahl-HS
SSBN-LS
SSBN-HS
E
*
Activation heat (kJ m-3)
Dahl-LS
Dahl-HS
SSBN-LS
SSBN-HS
F
Peak mechanical efficiency (%)
Dahl-LS
Dahl-HS
SSBN-LS
SSBN-HS